Odd-even staggering of the nuclear binding energy described by covariant density functional theory with calculations for spherical nuclei

Long Jun Wang (王龙军),[1] Bao Yuan Sun (孙保元),[1] Jian Min Dong (董建敏),[2] and Wen Hui Long (龙文辉)[1,*]

[1]*School of Nuclear Science and Technology, Lanzhou University, Lanzhou 730000, China*

[2]*Research Center for Nuclear Science and Technology, Lanzhou University and Institute of Modern Physics of CAS, Lanzhou 730000, China*

The odd-even staggerings (OESs) on nuclear binding energies are studied systematically within the spherical covariant density functional (CDF) theories, specifically the relativistic Hartree-Fock-Bogoliubov (RHFB) and the relativistic Hartree-Bogoliubov (RHB) theories. When taking the finite-range Gogny force D1S as an effective pairing interaction, both CDF models can provide appropriate descriptions on the OESs of nuclear binding energies for C, O, Ca, Ni, Zr, Sn, Ce, Gd, and Pb isotopes as well as for $N = 50$ and 82 isotones. While there still exist some systematical discrepancies from the data, i.e., the underestimated OESs in light C and O isotopes and the overestimated ones in heavy regions, respectively, such discrepancies can be eliminated partially by introducing a Z- or N-dependent strength factor into the pairing force Gogny D1S. As an example of application, distinct improvements are achieved with the optimized pairing force in determining the single-particle configurations of ^{112,114,118,124}Sn.

I. INTRODUCTION

In nuclear physics, the pairing mechanism is one of the basic ingredients in determining nuclear structure properties [1], and it becomes even more significant for exotic and superheavy nuclei, which have attracted wide interest from the community during recent decades [2–15]. Specifically in exotic nuclei [16], weakly bound nuclear systems under extreme conditions, crucial roles are played by the pairing correlations not only in predicting the isospin limits of finite nuclei [2–4] but also in developing the exotic modes, such as nuclear halo structures and possible Bardeen-Cooper-Schrieffer (BCS)–BEC crossover [5–9,14,15]. For superheavy nuclei with extra large charge numbers, many important properties such as nuclear shapes, fission barriers, and collective modes are essentially related with the effects of pairing [10–12].

Experimentally it is not so straightforward to measure the pairing effects, which are in general evaluated by the odd-even staggering (OES) on the nuclear binding energy. The binding energy of a system with an odd nucleon (neutron or proton) number is found to be lower than the arithmetic mean of two even neighbors, which leads to the so-called OES of single-nucleon separation energies along the isotopic or isotonic chains. Since the early days of nuclear physics, the OES was interpreted as the presence of pairing correlations between nucleons in a nucleus [1]. In the independent quasiparticle picture, the OES extracted from the experimental binding energies is often taken as the reference of the pairing-gap energy, which also provides a quantitative observable to constrain the pairing interaction [17].

During recent decades, many successes have been achieved by the covariant density functional (CDF) theories in describing the structural properties of nuclear systems [18–24].

One of the most popular CDF models is the relativistic Hartree approach with the no-sea approximation, namely, the relativistic mean field (RMF) theory [25,26], which has been widely applied in exploring the properties of both ground states [19,21,22] and excited states [21,27] for the finite nuclei in and far from the valley of β stability. However, due to the limit of the approach itself, significant system degrees of freedom are missing in RMF, such as the one-pion exchange [28] and ρ-tensor couplings. With the growth of computational facilities and the development of new methods, such defects can be eliminated with the inclusion of exchange (Fock) terms, which leads to a new CDF model—the density-dependent relativistic Hartree-Fock (DDRHF) theory [23] and its natural extension, the relativistic Hartree-Fock-Bogoliubov (RHFB) theory [29]. Besides compatible quantitative accuracy as RMF in describing nuclear bulk properties, substantial improvements are also achieved by DDRHF in the self-consistent description of nuclear shell structures and the evolutions [24,30–34], the relativistic symmetry restoration [35–37], the excitation modes [38], and neutron star physics [39,40].

In general the pairing effects in open-shell nuclei are considered within the BCS or Bogoliubov schemes. For a stable nuclear system, the BCS method can provide an efficient and simple way to handle the pairing correlations, although it meets serious problems when going beyond the stable region, especially when the halos emerge [22]. Approaching the nuclear isospin limits, the single neutron or proton separation energy becomes comparable to the pairing-gap energy such that the continuum can be involved easily by the pairing correlations. In terms of Bogoiubov quasiparticles, both mean field and pairing correlations are unified into the Bogoliubov scheme such that the continuum effects can be naturally taken into account. Aiming at the weakly bound nuclear systems, the CDF models combined with Bogoliubov framework have been extended as the relativistic Hartree-Bogoliubov (RHB) theory [21,41] and the RHFB theory [29]. Compared to the former, the RHFB theory provides a more concrete platform

*longwh@lzu.edu.cn

to evaluate the pairing effects due to the improvements brought by the Fock terms, especially with the inclusion of ρ-tensor couplings [24].

Besides the self-consistent treatment of the continuum effects, e.g., by the Bogoliubov theory, the theoretical reliability in describing the pairing effects also depends on the adopted pairing interaction. In the realistic calculations the particle-particle (pp) pairing interactions are usually taken as a phenomenological form, such as zero-range δ forces or finite-range Gogny interactions with great success in the relativistic and nonrelativistic calculations [22,29,42,43]. Due to its numerical simplicity, the δ-type forces are popularly applied in dealing with the pairing effects, especially when a realistic density dependence is introduced [44]. While limited by the zero-range formalism, it may require a sophisticated energy cutoff to decide the pairing window, as well as the strength of pairing interaction [44]. In contrast to the simple δ force, the finite-range Gogny forces have been widely taken as the effective interactions not only in the pp channels but also in the particle-hole (ph) channels and potentially better systematics is expected for the pp interaction. In addition to the benefit from the characteristic finite range, a natural energy cutoff is already embedded in modeling the pairing space. While it should be noticed that the pairing parts of Gogny forces were adjusted under the nonrelativistic approach [43,45,46], the global feasibility associated with the relativistic scheme [47,48] is still required to be tested, especially when the Fock terms are included in the ph channels. In fact, the CDF effective interactions have been attempted to unify the descriptions of both ph and pp channels in nuclear matter, while an effective factor has to be introduced in the pairing part to get reasonable gap parameters [49,50].

In this work, the OESs on nuclear binding energy will be systematically studied under the CDF scheme, specifically the RHFB and RHB theories. The content is organized as follows. In Sec. II, we briefly introduce the general formalism of the RHFB theory with finite-range Gogny pairing force. The neutron OESs along the isotopic chains of C, O, Ca, Ni, Zr, Sn, Ce, Gd, and Pb and the proton ones along the isotonic chains of $N = 50$, 82 are discussed systematically in Sec. III, as well as the effects with modified pairing strength. Finally, the summary is given in Sec. IV.

II. THEORETICAL FORMALISM AND NUMERICAL DETAILS

As commonly recognized, the nucleon-nucleon interaction in nuclear system is mediated by the exchange of mesons and photons. Standing on this criterion, the CDF model Lagrangian, i.e., the theoretical starting point, is constructed by including the degrees of freedom associated with the nucleon (ψ), the isoscalar σ and ω mesons, the isovector ρ and π mesons, and the photons (A) [51]. Following the standard variational procedure, the system Hamiltonian H is then determined as well as the field equations for nucleons, mesons, and photons, respectively the Dirac, Klein-Gordon, and Proca equations [26,51].

Standing on the level of mean field approach, the contributions of the negative-energy states are generally neglected, i.e., the so-called no-sea approximation. The CDF energy functional is then determined by the expectation of the system Hamiltonian H with respect to the Hartree-Fock ground $|\Phi_0\rangle$,

$$E = \langle\Phi_0|H|\Phi_0\rangle, \quad |\Phi_0\rangle = \prod_{i=1} c_i^\dagger |0\rangle, \tag{1}$$

where the index i denotes the states with positive energy and $|0\rangle$ is the vacuum state. Within the RHB theory, the energy functional (1) contains only the Hartree contributions, whereas both Hartree and Fock terms are included explicitly in the RHFB theory [29,41].

In the spherical system, the variation of the energy functional (1) with respect to the Dirac spinor $\psi(\boldsymbol{r})$ leads to the relativistic Hartree-Fock (RHF) equation as

$$\int d\boldsymbol{r}' h(\boldsymbol{r}, \boldsymbol{r}')\psi(\boldsymbol{r}') = \epsilon\psi(\boldsymbol{r}), \tag{2}$$

where ϵ is the single-particle energy and $h(\boldsymbol{r}, \boldsymbol{r}')$ denotes the single-particle Hamiltonian [29]. By combining the Bogoliubov transformation [52] with CDF models, the above RHF equation can be extended into the RHFB one [49] as

$$\int d\boldsymbol{r}' \begin{pmatrix} h(\boldsymbol{r}, \boldsymbol{r}') & \Delta(\boldsymbol{r}, \boldsymbol{r}') \\ -\Delta(\boldsymbol{r}, \boldsymbol{r}') & h(\boldsymbol{r}, \boldsymbol{r}') \end{pmatrix} \begin{pmatrix} \psi_U(\boldsymbol{r}') \\ \psi_V(\boldsymbol{r}') \end{pmatrix}$$
$$= (\gamma^0 E_q + \lambda) \begin{pmatrix} \psi_U(\boldsymbol{r}) \\ \psi_V(\boldsymbol{r}) \end{pmatrix}, \tag{3}$$

where ψ_U and ψ_V are the quasiparticle spinors, E_q denotes the quasiparticle energy, and the chemical potential λ is introduced to preserve the particle number on the average. In the single-particle Hamiltonian $h(\boldsymbol{r}, \boldsymbol{r}')$, the retardation effects are neglected as is usually done in mean field calculations [29]. The pairing potential $\Delta(\boldsymbol{r}, \boldsymbol{r}')$ in Eq. (3) reads as

$$\Delta_{\alpha\alpha'}(\boldsymbol{r}, \boldsymbol{r}') = -\frac{1}{2} \sum_{\beta\beta'} V_{\alpha\alpha'\beta\beta'}^{pp}(\boldsymbol{r}, \boldsymbol{r}')\kappa_{\beta\beta'}(\boldsymbol{r}, \boldsymbol{r}'), \tag{4}$$

with the pairing tensor [41]

$$\kappa_{\beta\beta'}(\boldsymbol{r}, \boldsymbol{r}') = \psi_{V_\beta}(\boldsymbol{r})^* \psi_{U_{\beta'}}(\boldsymbol{r}'). \tag{5}$$

For the pp interaction V^{pp} in Eq. (4), the following finite-range Gogny force is adopted in this work:

$$V(\boldsymbol{r}, \boldsymbol{r}') = \sum_{i=1,2} e^{[(r-r')/\mu_i]^2}(W_i + B_i P^\sigma - H_i P^\tau - M_i P^\sigma P^\tau),$$
$$\tag{6}$$

where μ_i, W_i, B_i, H_i, and M_i are the parameters of Gogny pairing force.

Except for few special cases, e.g., the RHB model with zero-range pairing force, the RHFB equation (3) is generally in an integro-differential form, which is difficult to solve efficiently in the coordinate space. In this work, the Dirac Woods-Saxon (DWS) basis [53], which can provide appropriate asymptotical behavior for the continuum states, is introduced to solve such integro-differential equation. For further details, the readers are referred to Ref. [29].

To evaluate the pairing effects, the following three-point indicators [54,55] of the OES of nuclear binding energies are introduced for isotopes (ν) and isotones (π), respectively:

$$\Delta_\nu^{(3)}(N) \equiv \frac{(-1)^N}{2}[S_n(N, Z) - S_n(N+1, Z)], \quad (7a)$$

$$\Delta_\pi^{(3)}(Z) \equiv \frac{(-1)^Z}{2}[S_p(N, Z) - S_p(N, Z+1)], \quad (7b)$$

where $\Delta_\nu^{(3)}(N)$ and $\Delta_\pi^{(3)}(Z)$ represent neutron (ν) and proton (π) OES, i.e., the difference on single-nucleon separation energies S_n (or S_p) of two neighboring isotopes (or isotones). Quantitatively there also exist other higher order indicators to evaluate the pairing effects, such as the four-point formula or the five-point ones [54]

$$\Delta_\nu^{(5)}(N) \equiv \frac{(-1)^N}{8}[S_n(N+2, Z) - 3S_n(N+1, Z)$$
$$+ 3S_n(N, Z) - S_n(N-1, Z)], \quad (8a)$$

$$\Delta_\pi^{(5)}(Z) \equiv \frac{(-1)^Z}{8}[S_p(N, Z+2) - 3S_p(N, Z+1)$$
$$+ 3S_p(N, Z) - S_p(N, Z-1)]. \quad (8b)$$

However, these higher order indicators may get the mean-field features involved, which may partially smooth out the odd-even oscillations due to the pairing effects [55]. Even with the three-point one (7), the obtained OESs for the isotopes (isotones) with even neutron (proton) number are still sensitive to both pairing and mean-field effects [55–57]. In order to avoid the disturbances of the mean field as much as possible, here we take only the OESs [see Eq. (7)] of the isotopes (isotones) with odd neutron (proton) number as the representatives to study the pairing effects.

To have an overall understanding on the pairing properties, we performed the calculations within both RHFB and RHB for the C, O, Ca, Ni, Zr, Sn, Ce, Gd, and Pb isotopes, and $N = 50$ and 82 isotones, from which are extracted the neutron and proton OESs by Eq. (7) for the odd isotopes or isotones. In all the calculations, the pp interaction V^{pp} is taken as the finite-range Gogny force D1S [58]. In the ph channel, we adopt four CDF effective interactions with density-dependent meson-nucleon couplings, i.e., PKA1 [24], PKO3 [30], PKDD [59], and DD-ME2 [60]. For the RHB calculations with PKDD and DD-ME2, only the Hartree contributions are involved, whereas both Hartree and Fock terms are taken into account by the RHFB ones with PKA1 and PKO3. Due to the limit of the approach itself, the π and ρ tensor couplings are missing in PKDD and DD-ME2, while PKO3 contains the π couplings and both are involved in PKA1. It was proved that the inclusion of the Fock terms and correspondingly the π- and ρ-tensor couplings play essential roles in improving the self-consistent descriptions of shell evolution and single-particle structures [24,30,31].

It should be mentioned that both RHFB and RHB calculations are restricted to the level of the mean field approach with spherical symmetry for the selected isotones and isotopes, and the effects of deformation are neglected in the present work. Currently the integro-differential RHFB equation (3) is solved by expanding the quasiparticle spinors ψ_U and ψ_V on the Dirac Woods-Saxon (DWS) basis [29,53]. It is checked

to be accurate enough to take the parameters of the DWS basis as $R_{\max} = 20$ fm, $N_F = 28$, and $N_D = 12$, where $R_{\max}$ is the size of the spherical box and $N_F(N_D)$ corresponds to the numbers of positive- (negative-) energy states included in the basis expansion.

For the nuclei with odd neutron and/or proton numbers, the blocking configurations are utilized here to approximate the odd-nucleon effects. Practically, by blocking different orbits around the Fermi surface, the configuration with the strongest binding is determined as the ground state. Notice that in the odd nuclei the time reverse symmetry is broken due to the odd nucleon. However, in this work we neglect the current effects since the mean field would not be essentially changed by the odd particle [61–63].

III. RESULTS AND DISCUSSION

A. Odd-even staggering along the isotopic and isotonic chains

We first study the neutron OESs of the selected isotopes with odd neutron number within the RHFB and RHB theories. Figure 1 shows the evolution of neutron OESs $\Delta_\nu^{(3)}(N)$ (in open symbols) along the isotopic chains of C, O, Ca, Ni, Zr, Sn, Ce, Gd, and Pb, where the experimental data (in filled squares) extracted from Ref. [64] are presented as the reference. The theoretical results are provided by the calculations with PKA1, PKO3, and PKDD. The results from DD-ME2 are omitted because they show similar systematics as PKDD on the OESs. It is clearly seen that all the calculations with selected effective interactions can provide appropriate overall agreement with the data to certain extent.

For the light nuclei, PKA1 shows better agreement with the data than PKO3 and PKDD on the isospin evolution of OESs along the isotopic chain of carbon. For O isotopes, the experimental depressions of neutron OESs $\Delta_\nu^{(3)}(N)$ at $N = 7$ and $N = 15$ are qualitatively reproduced by all the theoretical calculations, consistent with the occurrences of the shell structures at $N = 8$ and 16. However, quantitatively all the theoretical calculations underestimate the OESs at the proton-rich sides. The possible reason could be the missing of the correlations beyond the mean-field level. It has been noticed that an enhancement of the pairing correlations could occur when the particle-vibration coupling is included beyond the mean field, which is expected to affect the single-particle energy in odd-mass nuclei [65–70]. The present work does not include such coupling, but the corresponding effects are found to about 1/7 on shell gaps [71] and accordingly about 1/14 on OES (see Eq. (7) of Ref. [56]). Moreover, the discrepancies as seen at $N = 7$ on the OESs for both C and O isotopes might be partly due to the pairing collapse phenomenon in the related regions of phase transitions (i.e., close to the magic configurations) [72], which could be cured theoretically by the particle-number projection [73]. It should also be noticed that the selected C and O isotopes have reached the neutron dripline, where the continuum can be involved substantially. In Ref. [34], the consistent relation between the continuum effects and the OES on the neutron radius has been illustrated for the carbon isotopes, whereas for oxygen the contributions from the continuum are fairly tiny due to the occurrence of magic shell $N = 16$ [74].
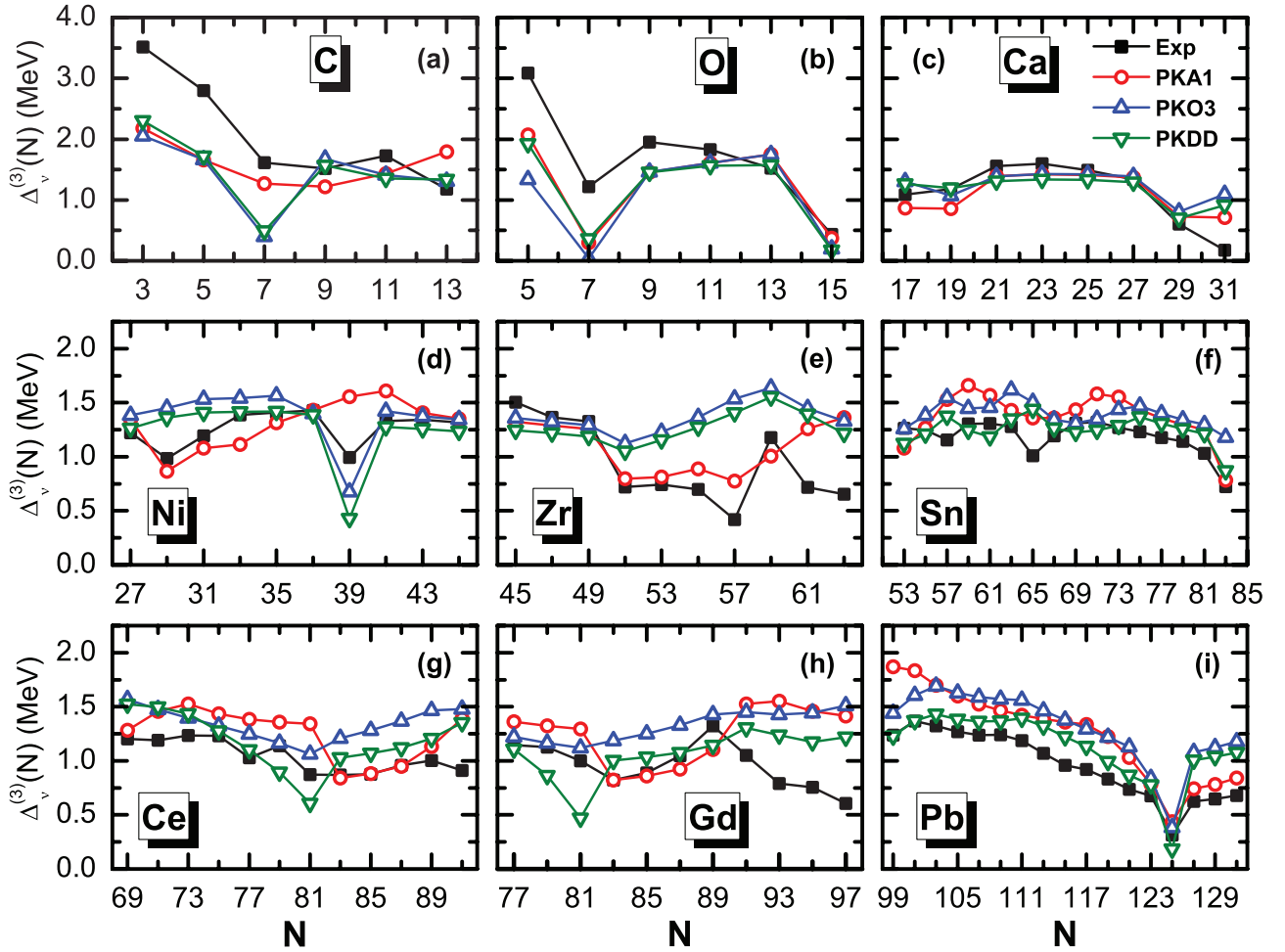
FIG. 1. (Color online) Neutron OESs $\Delta_\nu^{(3)}(N)$ [see Eq. (7)] as functions of neutron number N for the C, O, Ca, Ni, Zr, Sn, Ce, Gd, and Pb isotopes. The results are extracted from the calculations of RHFB with PKA1 (in open circles) and PKO3 (in open upward-pointing triangles), and RHB with PKDD (in open downward-pointing triangles), in comparison with the data [64] (in filled squares). The finite-range Gogny force D1S is utilized as the effective pairing force. See the text for details.

For the medium-heavy nuclei it is found that the neutron OESs of Ca isotopes are precisely reproduced by PKA1, PKO3, and PKDD except the one at $N = 31$. For Ni isotopes, PKA1, PKO3, and PKDD also present proper overall agreements, except $N = 29$ for PKO3 and PKDD and $N = 39$ for all the selected effective interactions. From the consistent relation between the pairing effects and shell structures, it seems that the shell effect around $N = 28$ is underestimated by PKO3 and PKDD, whereas the one at $N = 40$ is underestimated by PKA1 and overestimated by PKO3 and PKDD. For Zr isotopes, the neutron OESs are described precisely by PKA1 until the distinct discrepancies occur beyond $N = 59$, where the nuclei may be deformed [75]. In contrast, PKO3 and PKDD present remarkable deviations from the data in a fairly wide range since $N > 49$. The model deviations in reproducing the neutron OESs here may be connected with the fact that PKA1, in which the ρ-tensor coupling is included [24], provides better descriptions on the nuclear shell structures and therefore improved consistence with the pairing effects, as mentioned previously.

For heavier nuclei, e.g., the Sn isotopes, the experimental OESs $\Delta_\nu^{(3)}(N)$ keep around the value of 1.2 MeV, except

at $N = 65$ and $N = 83$. Quantitatively PKDD provides the best agreement with the data while the neutron OESs are slightly overestimated by PKA1 and PKO3. For Ce and Gd isotopes, although some of them may be deformed [75], the spherical calculations with PKA1, PKO3, and PKDD still provide appropriate descriptions on the neutron OESs, except for Gd isotopes beyond $N = 89$. This is perhaps because the effects of deformation could be canceled in Eq. (7) to some extent since the three adjacent nuclei in the three-point indicators share nearly the same deformation [75]. Along the isotopic chain of Pb, the systematics of neutron OESs are properly described by PKA1, PKO3, and PKDD, while there still exists some systematical overestimation.

Concerning the evolutions of proton OESs along the isotonic chains of $N = 50$ and 82, similar systematics are also obtained from the CDF calculations with PKA1, PKO3, and PKDD, as referred to the data [64]. From Figs. 2(a) and 2(c) it is seen that the proton OESs for $N = 50$ and 82 isotones are reproduced in an appropriate agreement with data by the selected effective interactions. In particular, the calculations with both PKA1 and PKO3 present the clear depression of
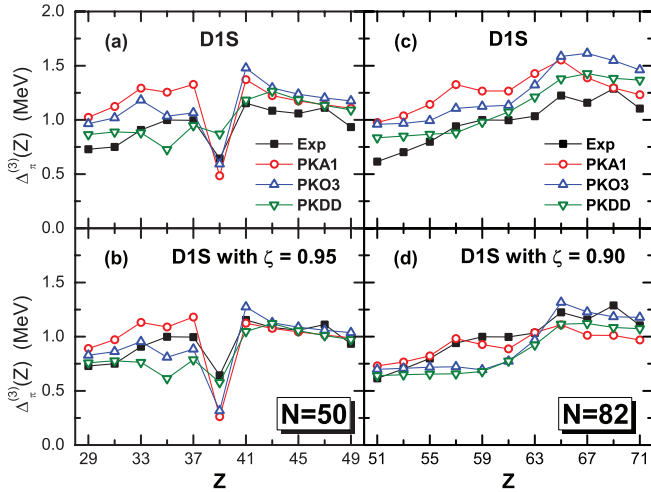
FIG. 2. (Color online) Proton OESs $\Delta_\pi^{(3)}(Z)$ of $N = 50$ and 82 isotones as functions of proton number Z. The results are calculated by the RHFB theory with PKA1 and PKO3 and by the RHB theory with PKDD, where the Gogny force D1S is utilized in the pairing channel. The experimental data extracted from Ref. [64] are also shown for comparison. The results without and with the effective pairing strength factor ζ are shown in the upper [(a) and (c)] and lower [(b) and (d)] panels respectively.

$\Delta_\pi^{(3)}(Z)$ at $Z = 39$ for $N = 50$ isotones, corresponding with the subshell structure $Z = 40$, which may imply the extra role of Fock terms, especially the embedded tensor effects, in determining the nuclear shell structure for the selected isotonic chain [33]. Compared to the data quantitatively, however, the pairing effects are also somewhat overestimated for the selected isotones. It is worthwhile to mention that the calculations with other relativistic effective Lagrangian, e.g., the RHB with DD-ME2 [60], also show a similar trend. In brief one may reach the point that the OESs, coherently the pairing effects, are somewhat underestimated by the CDF

calculations for light nuclei and overestimated for heavy nuclei.

In general the statistical observables, i.e., the root-mean-square (rms) deviation $\sigma_{\rm rms}$ and the average one $\mathcal{D}$ from the data, are introduced to test quantitative precision of the theoretical calculations,

$$\sigma_{\rm rms} = \sqrt{\frac{1}{n} \sum_{i=1}^{n} \left| \Delta_{i,{\rm Cal}}^{(3)} - \Delta_{i,{\rm Exp}}^{(3)} \right|^2}, \tag{9}$$

$$\mathcal{D} = \frac{1}{n} \sum_{i=1}^{n} \left[\Delta_{i,{\rm Cal}}^{(3)} - \Delta_{i,{\rm Exp}}^{(3)} \right], \tag{10}$$

where $\Delta_{i,{\rm Cal}}^{(3)}$ and $\Delta_{i,{\rm Exp}}^{(3)}$ denote the OESs extracted from the CDF calculations and the experimental data, respectively, and n is the number of odd isotopes (isotones) in the selected isotopic (isotonic) chains. Table I shows the values of $\sigma_{\rm rms}$ and $\mathcal{D}$ for the selected isotopes and isotones. It is found that the calculations with PKA1, PKO3, and PKDD present negative average error $\mathcal{D}$ for C and O isotopes and positive ones for nuclei heavier than Ni isotopes. Such systematics may also indicate that the pairing effects are somehow underestimated for light nuclei and overestimated for heavy nuclei by taking the finite-range Gogny force D1S as the effective pairing interaction, which has already been demonstrated from the results in Figs. 1, 2(a), and 2(c).

To eliminate such systematical discrepancy with the data, additional strength factor ζ is introduced into the pairing interaction, as in Ref. [47],

$$V_{\rm opt}^{\rm pp}(\boldsymbol{r}, \boldsymbol{r}') = \zeta V^{\rm pp}(\boldsymbol{r}, \boldsymbol{r}'), \tag{11}$$

where $V^{\rm pp}(\boldsymbol{r}, \boldsymbol{r}')$ and $V_{\rm opt}^{\rm pp}(\boldsymbol{r}, \boldsymbol{r}')$ are the original and optimized pairing force. The optimized strength factor ζ is determined with respect to the root-mean-square deviation $\sigma_{\rm rms}$ from the PKA1 calculations with different values of ζ since PKA1 can better describes the nuclear structure properties [24]. As examples, Fig. 3 shows the neutron OESs of Sn and Pb isotopes calculated with the optimized Gogny pairing

TABLE I. The root-mean-square deviation $\sigma_{\rm rms}$ and the average error $\mathcal{D}$ of OES for the isotopes C, O, Ca, Ni, Zr, Sn, Ce, Gd, and Pb and for the isotones $N = 50$ and 82, determined by the CDF calculations with PKA1, PKO3, and PKDD. The results inside (outside) the parentheses are presented by the calculations taking the Gogny force D1S with (without) pairing strength factor ζ as the effective pairing interaction. See the text for details.

|	ζ	$\sigma_{\rm rms}$			$\mathcal{D}$		
		PKA1	PKO3	PKDD	PKA1	PKO3	PKDD
C	1.20	0.792(0.665)	0.916(0.816)	0.824(0.671)	$-0.467(-0.125)$	$-0.640(-0.203)$	$-0.597(-0.159)$
O	1.15	0.609(0.582)	0.899(0.649)	0.641(0.594)	$-0.415(-0.173)$	$-0.609(-0.100)$	$-0.498(-0.173)$
Ca	1.00	0.255	0.354	0.305	-0.032	$+0.109$	$+0.039$
Ni	1.00	0.230	0.228	0.230	$+0.046$	$+0.108$	-0.014
Zr	1.00	0.323	0.577	0.511	$+0.128$	$+0.393$	$+0.295$
Sn	0.95	0.230(0.135)	0.257(0.145)	0.158(0.167)	$+0.186(+0.043)$	$+0.211(-0.085)$	$+0.062(+0.035)$
Ce	0.93	0.266(0.155)	0.332(0.176)	0.241(0.184)	$+0.205(-0.002)$	$+0.294(+0.083)$	$+0.132(-0.037)$
Gd	0.90	0.447(0.339)	0.452(0.251)	0.338(0.314)	$+0.281(-0.002)$	$+0.362(+0.056)$	$+0.098(-0.160)$
Pb	0.90	0.327(0.118)	0.362(0.122)	0.218(0.163)	$+0.296(+0.049)$	$+0.344(+0.057)$	$+0.167(-0.088)$
$N = 50$	0.95	0.250(0.172)	0.204(0.137)	0.148(0.148)	$+0.196(+0.037)$	$+0.171(-0.011)$	$+0.062(-0.079)$
$N = 82$	0.90	0.300(0.123)	0.287(0.147)	0.163(0.171)	$+0.278(-0.055)$	$+0.269(-0.061)$	$+0.127(-0.135)$
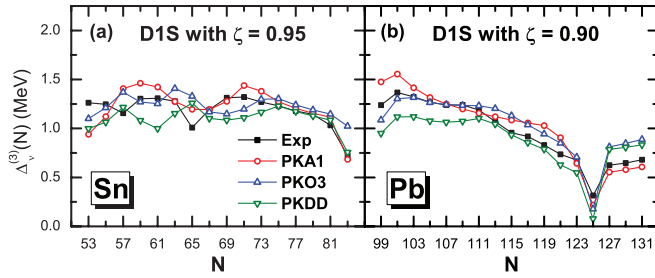
FIG. 3. (Color online) The same as Fig. 1 but for Sn (a) and Pb (b) isotopes calculated by the optimized Gogny pairing force D1S with the effective pairing factor ζ. See the text for details.

force D1S, in which the strength factor ζ are respectively taken as 0.95 and 0.90. By comparing the results with original pairing force (i.e., $\zeta = 1.0$) in Figs. 1(f) and 1(i), one can see that the agreements with the data are remarkably improved by the inclusion of the strength factor. In Ref. [48] similar conclusions have also been reached in reproducing the experimental data of inertia moments for very heavy nuclei. For the $N = 50$ and 82 isotones, as shown in Figs. 2(b) and 2(d), the systematical overestimation on proton OESs can be also eliminated by reducing the strength factors as $\zeta = 0.95$ and 0.90, respectively.

In fact, such improvements can be demonstrated quantitatively from the statistical observables in Table I for all the selected isotopes and isotones. It is shown that with the inclusion of the strength factor almost all the CDF calculations present nearly zero average deviations $\mathcal{D}$, especially for the heavy isotopes and isotones, which corresponds to an improvement of the systematics of pairing effects. As shown in the second column of Table I, the strength factors ζ represent distinct Z dependence for isotopes, as well as N dependence for isotones; i.e., ζ decreases monotonically with increasing proton number Z of the isotopes or neutron number N of the isotones, consistent with the systematic deviations as seen from Figs. 1 and 2. As seen from rms deviations in Table I, remarkable improvements on the agreements can be also found with the inclusion of the strength factor in pp interaction. For the neutron OESs the statistic qualities of the agreements, i.e., the values of σ_{rms}, are improved by about 10% for light nuclei (C and O) and about 30% for heavy ones (Sn, Ce, Gd, and Pb), whereas for the isotones of $N = 50$ and $N = 82$ (the last two rows in Table I), the RHFB calculations with optimized pairing forces respectively present about 30% and 50% improvement on the rms deviations σ_{rms}, which are almost unchanged in the RHB calculations with PKDD as well as with DD-ME2.

Figure 4 presents the proton effective pairing gaps of the $N = 50$ (left plots) and 82 (right plots) isotones with even proton numbers, i.e., the average gap energies extracted from the RHFB calculations (see Eq. (5.5) of Ref. [42]). For comparison, the OESs of the experimental binding energies are shown by three-point (filled squares) and five-point (filled circles) indicators. As the experimental reference of pairing effects, one may find distinct deviations between these two formalisms along the isotonic chain of $N = 50$ [see Fig. 4(a)] and such deviations become smaller for $N = 82$ isotones. This
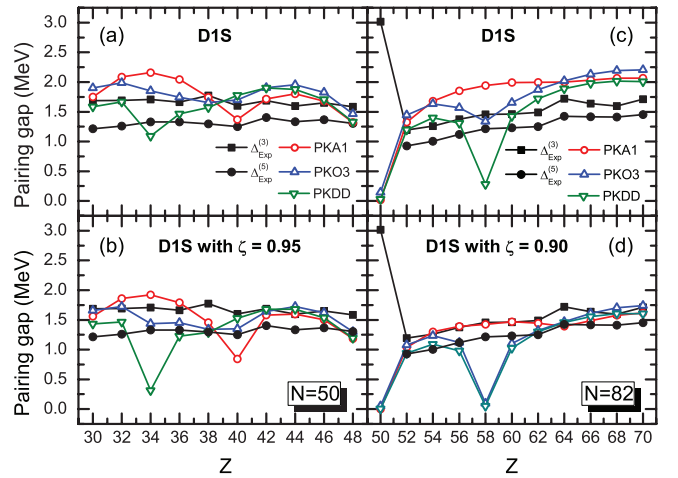

FIG. 4. (Color online) The average proton pairing gap of $N = 50$ and $N = 82$ even isotones compared with the corresponding proton OES extracted from the data [64]. The results without and with the effective pairing strength factor ζ are shown in the left [(a) and (c)] and right [(b) and (d)] panels respectively. See the text for details.

is mainly due to the fact that these evaluations of pairing effects for even-even nuclei have already got the mean-field effects involved to different extents [55,56]. As referred to the experimental values, the calculated effective pairing gaps still show appropriate agreements, especially for the calculations with optimized pairing force by the three-point indicator, which agree with the conclusion that the OES of three-point indicator can well describe the average pairing gap instead of higher order indicators [56]. It should be noticed that along the isotonic chain of $N = 50$ the calculations with PKA1 present distinct depression at $Z = 40$, which implies the occurrence of some subshell closures, also demonstrated by the OES depression of the odd isotones at $Z = 39$ [see Figs. 2(a) and 2(b)]. The calculations with PKO3 and PKDD do not show similar consistencies between the results of odd and even isotones; e.g., for the odd $N = 50$ isotones the OES results show certain depression at $Z = 39$ [see Figs. 2(a) and 2(b)], whereas the effective pairing gaps for the even isotones are just changed smoothly at $Z = 40$ [see Figs. 4(a) and 4(b)]. Along the isotonic chain of $N = 82$, the inconsistencies are also observed at $Z = 58$ from the results of PKO3 and PKDD; i.e., the values of the effective pairing gaps clearly indicate the existence of the artificial shell closure $Z = 58$ [24,76] while such spurious shell is not found from the systematics on the OESs of the odd isotones.

B. NUCLEAR STRUCTURE PROPERTIES WITH OPTIMIZED PAIRING FORCE

Since substantial improvements in reproducing the neutron and proton OESs have been achieved with the optimized pairing force $V_{\mathrm{opt}}^{\mathrm{pp}}$ [see Eq. (11)], it is worthwhile to test the relevant effects in describing the nuclear structure properties, such as the single-particle configurations, pairing energies, and nuclear binding energies. As a direct response, the occupation probabilities of valence orbits will be essentially changed with

TABLE II. Occupation numbers of valence neutron orbits in ^{112,114,118,124}Sn, calculated by RHFB with PKA1 and PKO3, and by RHB with PKDD and DD-ME2, in comparison with the data [77,78]. In the calculations, the pairing force is adopted as the original Gogny D1S and the optimized one with $\zeta = 0.95$ (inside the parentheses), respectively. The bold types denote the theoretical results within the error bars of the data. See the text for details.

Orbit		^{112}Sn					^{114}Sn			
	Exp.	PKA1	PKO3	PKDD	DD-ME2	Exp.	PKA1	PKO3	PKDD	DD-ME2
$\nu 2d_{5/2}$	0.93 ± 0.12	**0.82(0.84)**	0.61(0.63)	0.61(0.62)	0.65(0.66)	0.97 ± 0.09	0.86(**0.88**)	0.73(0.76)	0.759(0.80)	0.80(0.83)
$\nu 1g_{7/2}$	0.63 ± 0.13	**0.55(0.56)**	0.83(0.86)	0.89(0.91)	0.86(0.88)	0.69 ± 0.15	**0.65(0.67)**	0.88(0.90)	0.923(0.94)	0.91(0.94)
$\nu 3s_{1/2}$	0.24 ± 0.03	0.31(0.30)	0.14(0.12)	0.09(0.07)	0.11(0.09)	0.34 ± 0.03	0.41(0.41)	0.22(0.19)	0.16(0.14)	0.19(0.16)
$\nu 2d_{3/2}$	0.18 ± 0.025	0.31(0.29)	**0.19(0.16)**	0.12(0.10)	0.15(0.12)	0.37 ± 0.04	**0.40(0.39)**	0.27(0.25)	0.20(0.17)	0.23(0.20)
$\nu 1h_{11/2}$		0.08(0.06)	0.06(0.05)	0.05(0.04)	0.04(0.03)	0.25 ± 0.07	0.10(0.09)	0.09(0.07)	0.08(0.06)	0.05(0.04)

Orbit		^{118}Sn					^{124}Sn			
	Exp.	PKA1	PKO3	PKDD	DD-ME2	Exp.	PKA1	PKO3	PKDD	DD-ME2
$\nu 2d_{5/2}$	1.00 ± 0.10	**0.91(0.93)**	0.86(0.89)	**0.88(0.90)**	**0.92(0.94)**	1.00 ± 0.09	**0.96(0.97)**	**0.94(0.95)**	**0.95(0.96)**	**0.96(0.97)**
$\nu 1g_{7/2}$	0.78 ± 0.19	**0.81(0.83)**	**0.93(0.94)**	**0.95(0.96)**	**0.96(0.97)**	0.81 ± 0.23	**0.93(0.94)**	**0.96(0.97)**	**0.97(0.98)**	**0.98(0.98)**
$\nu 3s_{1/2}$	0.80 ± 0.10	0.65(0.67)	0.45(0.45)	0.40(0.40)	1.00(1.00)	0.95 ± 0.10	**0.88(0.90)**	0.77(0.78)	0.73(0.74)	**1.00(1.00)**
$\nu 2d_{3/2}$	0.60 ± 0.08	**0.61(0.62)**	0.52(0.52)	0.46(0.46)	0.56(0.58)	0.75 ± 0.10	**0.85(0.87)**	**0.81(0.82)**	**0.77(0.78)**	**0.86(0.88)**
$\nu 1h_{11/2}$	0.35 ± 0.08	0.17(0.16)	0.20(0.18)	0.20(0.18)	0.13(0.10)	0.38 ± 0.12	**0.46(0.44)**	**0.47(0.46)**	**0.49(0.48)**	**0.43(0.42)**

the modifications of the pairing strength, as well as the pairing energies.

In Table II are shown the calculated occupation probabilities of neutron valence orbits $2d_{5/2}$, $1g_{7/2}$, $3s_{1/2}$, $2d_{3/2}$, and $1h_{11/2}$ in ^{112}Sn, ^{114}Sn, ^{118}Sn, and ^{124}Sn, as compared to the data taken from Refs. [77,78]. The bracketed numbers are the results calculated with the optimized pairing force V_{opt}^{pp} ($\zeta = 0.95$). Among the selected effective Lagrangians, PKA1 shows the best agreements with the data within the error bars (denoted by bold types), whereas lesser agreements are provided by the calculations with PKO3, PKDD, and DD-ME2, especially the improper order of the pseudospin partners $2d_{5/2}$ and $1g_{7/2}$. As seem from the data of occupation probabilities, the neutron orbit $2d_{5/2}$ is almost fully filled whereas $1g_{7/2}$ is just gradually occupied, which implies that $2d_{5/2}$ is bound deeper than $1g_{7/2}$ in the selected isotopes. Evidently PKA1 presents more reliable description on nuclear structures than the other selected effective Lagrangians.

In the PKA1 calculations the optimized pairing force V_{opt}^{pp} also bring some systematic improvements on the agreement with the data, i.e., being closer to the central values of the data, whereas with PKO3 and PKDD, such systematical improvements cannot be observed, which may be partially due to the inappropriate order of the valence orbits. If comparing the occupations of another pseudospin doublet $3s_{1/2}$ and $2d_{3/2}$, one may also find the improper order of these two states described by PKO3 and PKDD in ^{112,118,124}Sn and by DD-ME2 in ^{112}Sn. Compared with the distinct improvements on the OESs with V_{opt}^{pp}, the corresponding effects on the occupations are relatively weak because the configurations are determined not only by the pairing effects, but also more essentially by the concrete shell structure, in which the mean field plays the dominant role.

As another direct effect, the modification on the pairing interaction will substantially change the contributions from the pairing correlations to the energy functional. Taking the even Pb isotopes as the representatives, Table III shows the pairing energies from the RHFB and RHB calculations with the selected effective parameters. For comparison the results calculated by RHB with NL1 and by nonrelativistic

HFB with Gogny D1S are also shown [47]. It should be mentioned that in the former RHB-NL1 calculations the effective pairing interaction was taken as the Gogny force D1S with additional strength factor $\zeta = 1.15$, whereas for the latter Gogny calculations it kept as the original one [47].

As seen from Table III the pairing energies are remarkably reduced in the calculations of PKA1, PKO3, and PKDD with the optimized pairing force V_{opt}^{pp}, which leads to weaker pairing contributions than those from NL1 and Gogny calculations. In this work the pairing interaction is optimized as referred to the OESs of binding energies of the odd isotopes, while in Ref. [47] the strength factor $\zeta = 1.15$ is simply determined to reproduce the pairing energies of the Gogny calculations for Pb isotopes. Such deviations between the models may also originate from the inconsistency between the relativistic mean field and nonrelativistic pairing potential, as mentioned before. As referred to the pairing energies, the PKA1 and PKO3 calculations with original Gogny pairing force present slightly stronger pairing effects than the Gogny ones, while PKDD and DD-ME2 present much weaker pairing effects. This discrepancy between the RHF and RMF models can be interpreted by the values of the nonrelativistic-type effective mass [23,79]. With the inclusion of Fock terms, PKA1 and PKO3 have a fairly large effective mass, close to the nonrelativistic ones, whereas in general the RMF models present smaller effective masses, e.g., by PKDD and DD-ME2. Globally the level densities determined by PKA1 and PKO3 are then larger than PKDD and DD-ME2 such that stronger pairing effects are obtained by the former ones with the same pairing interaction. This may also partially explain the reason why we have different pairing strength factors from the previous NL1 calculations.

To provide a statistical understanding on the effects of the optimized pairing force, Figs. 5 and 6 show the statistic behaviors of the deviations from the experimental data for both binding energies and OESs, respectively. For comparison, the results calculated with the original and optimized Gogny pairing forces are respectively shown in the upper and lower panels. In these two figures the solid curves denote the

TABLE III. The pairing energy of Pb isotopes obtained by the CDF calculations with PKA1, PKO3, and PKDD. The results inside (outside) the parentheses are presented by the calculations taking the Gogny force D1S with (without) pairing strength factor ζ as the effective pairing interaction. The corresponding results of RHB theory with NL1 with $\zeta = 1.15$ and of HFB theory with Gogny force [47] are also shown for comparison.

| A	PKA1	PKO3	PKDD	NL1	Gogny
196	$-24.72(-17.76)$	$-24.54(-17.04)$	$-17.47(-11.62)$		
198	$-22.40(-16.03)$	$-22.40(-15.38)$	$-15.56(-10.14)$		
200	$-19.40(-13.73)$	$-19.52(-13.13)$	$-13.14(-8.34)$		
202	$-15.65(-10.83)$	$-15.86(-10.28)$	$-10.23(-6.26)$	-14.49	-14.41
204	$-11.14(-7.34)$	$-11.34(-6.85)$	$-6.85(-3.97)$	-10.41	-10.49
206	$-5.90(-3.50)$	$-6.00(-3.11)$	$-3.17(-1.48)$	-5.57	-5.74
208	$0.00(0.00)$	$0.00(0.00)$	$0.00(0.00)$	0.00	0.00
210	$-4.81(-2.93)$	$-6.89(-4.30)$	$-5.34(-3.66)$	-4.79	-4.19
212	$-8.58(-5.04)$	$-12.00(-7.67)$	$-9.61(-6.56)$	-8.66	-8.64
214	$-11.64(-6.37)$	$-16.04(-10.33)$	$-12.99(-8.87)$	-11.77	-12.89
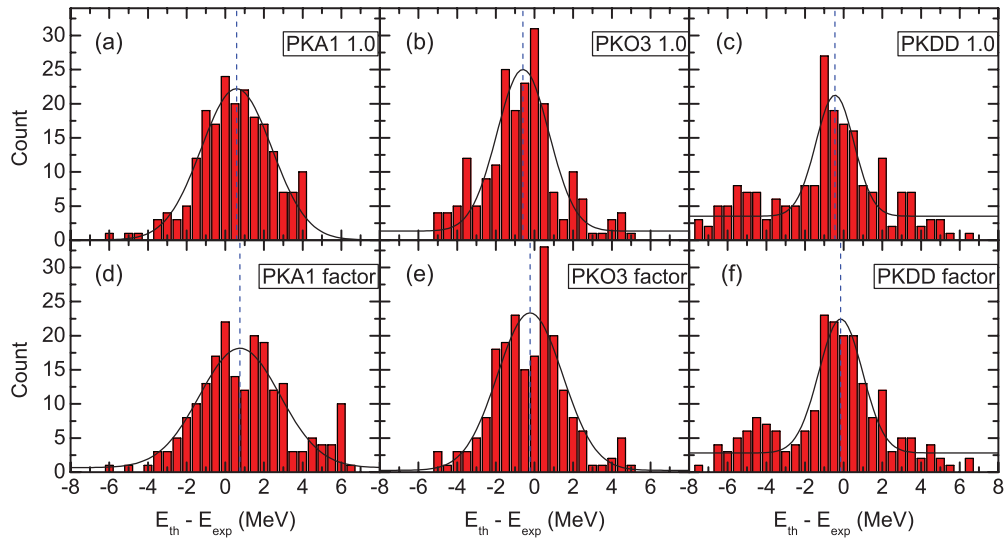
FIG. 5. (Color online) Distributions of deviations from experiment of the binding energies of 205 spherical nuclei in the selected isotopes and isotones (0.5-MeV bins). Results obtained without (with) the effective pairing strength factor are shown in the upper (lower) panels. The best-fitted Gaussian distributions [see Eq. (12)] are also shown with black lines, and the corresponding parameters are listed in Table IV.

Guassian statistic fittings as

$$y = y_0 + \frac{A}{w\sqrt{\pi/2}} e^{-2\frac{(x-x_c)^2}{w^2}}, \qquad (12)$$

where y_0 is the minimum counts, A represents the area of the Gaussian distribution, and x_c and w denote the statistic averages (ideally zero) and errors. In Figs. 5 and 6 it is clearly shown that the deviations of both binding energies and OESs from the data obey the Gaussian statistic behaviors. For the binding energy the deviations are not symmetrically distributed on the negative and positive sides and more counts are found for the positive deviations, mainly due to the deformation effects neglected in current calculations of Zr,

Ce, and Gd isotopes. It is expected to improve the results by including the deformation effects, which in general lead to more bound ground states. For the OESs the statistic distributions are nearly symmetric, especially for the PKA1 results with the optimized pairing force. Evident improvements due to the optimize pairing interaction can be also demonstrated from the statistic variables shown in Table IV. It is seen that the statistic averages and errors on the OES deviations, i.e., the values of x_c and w, are improved distinctly, while the improvements on the binding energies are not so distinct and systematical as the OESs. Especially for PKA1 the statistic qualities even become worse, inconsistent with the evident improvements on the OESs.
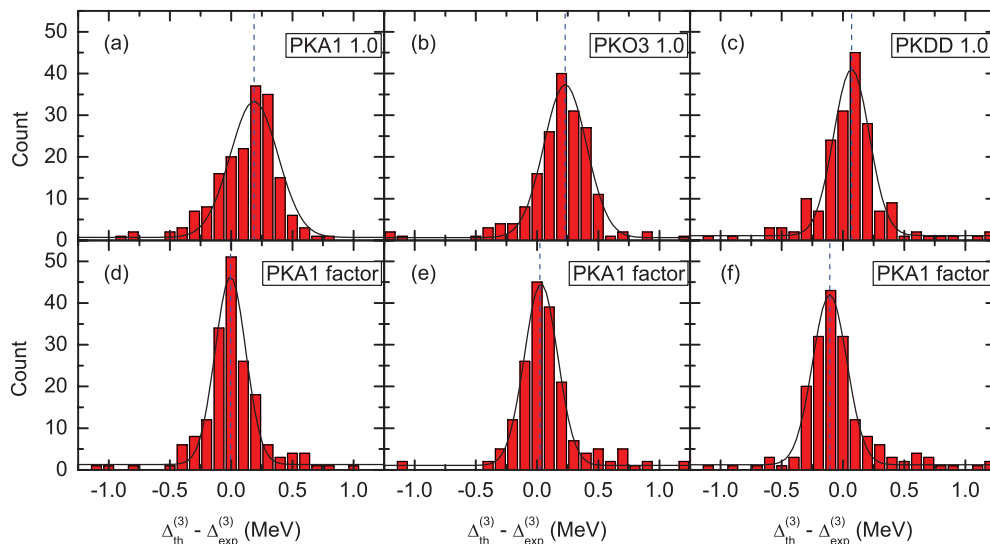

FIG. 6. (Color online) The same as Fig. 5 but for the OES [see Eq. (7)] of 186 spherical nuclei with both even and odd nucleon numbers in the selected isotopes and isotones (0.1-MeV bins).

TABLE IV. Parameters of the corresponding Gaussian distributions [see Eq. (12)] for the binding energy in Fig. 5 and the OES in Fig. 6. Results obtained without (with) the effective pairing strength factor are shown outside (inside) the parentheses.

	y_0	x_c	w	A
		Binding energy		
PKA1	0.05(0.66)	0.58(0.76)	3.65(4.16)	101.26(91.05)
PKO3	1.34(0.27)	-0.60(**0.23**)	2.69(3.37)	87.39(97.60)
PKDD	3.52(2.80)	-0.45(**0.15**)	1.97(**2.26**)	43.87(55.54)
		OES		
PKA1	0.73(1.31)	0.19($-$**0.01**)	0.39(**0.24**)	15.93(14.13)
PKO3	0.67(1.06)	0.23(**0.03**)	0.35(**0.27**)	16.02(14.80)
PKDD	1.15(1.23)	0.07(-0.10)	0.30(**0.28**)	14.52(14.30)

IV. SUMMARY

In summary, the neutron odd-even mass staggerings (OESs) of C, O, Ca, Ni, Zr, Sn, Ce, Gd, and Pb isotopes, and the proton ones of $N = 50$ and 82 isotones, are studied systematically within the spherical covariant density functional theory, specifically the relativistic Hartree-Fock-Bogoliubov (RHFB) theory with PKA1 and PKO3 and the relativistic Hartree-Bogoliubov (RHB) theory with PKDD and DD-ME2.

By taking the finite-range Gogny force D1S as an effective paring interaction, the neutronand proton OESs can be properly reproduced by the selected effective Lagragians. However, some systematic discrepancies with the data of the OESs are found, namely, the OESs and coherently the pairing effects are somewhat underestimated for light nuclei and overestimated for the heavy ones. Such discrepancies can be eliminated partially by introducing a Z- or N-dependent strength factor into the pairing force, which present better agreements with the experimental data of the OESs by improving the root-mean-square deviation σ_{rms} of the OES about 10% for light nuclei and 30% for heavy ones. Similar improvements are also obtained on the description of single-particle configurations, especially in the calculations with PKA1. In addition, the effects of the optimized pairing force on the pairing energy and binding energy are analyzed systematically.

[1] A. Bohr and B. R. Mottelson, *Nuclear structure* (World Scientific Publishing, Singapore, 1998), Vol. 1.
[2] D. Vretenar, G. A. Lalazissis, and P. Ring, Phys. Rev. C **57**, 3071 (1998).
[3] G. A. Lalazissis and S. Raman, Phys. Rev. C **58**, 1467 (1998).
[4] G. A. Lalazissis, D. Vretenar, W. Pöschl, and P. Ring, Nucl. Phys. A **632**, 363 (1998).
[5] J. Meng and P. Ring, Phys. Rev. Lett. **77**, 3963 (1996).
[6] J. Meng and P. Ring, Phys. Rev. Lett. **80**, 460 (1998).
[7] K. Hagino, H. Sagawa, J. Carbonell, and P. Schuck, Phys. Rev. Lett. **99**, 022506 (2007).
[8] B. Y. Sun, H. Toki, and J. Meng, Phys. Lett. B **683**, 134 (2010).
[9] T. T. Sun, B. Y. Sun, and J. Meng, Phys. Rev. C **86**, 014305 (2012).
[10] A. Sobiczewski and K. Pomorski, Prog. Part. Nucl. Phys. **58**, 292 (2007).
[11] S. Karatzikos, A. V. Afanasjev, G. A. Lalazissis, and P. Ring, Phys. Lett. B **689**, 72 (2010).
[12] G. A. Lalazissis, M. M. Sharma, P. Ring, and Y. K. Gambhir, Nucl. Phys. A **608**, 202 (1996).
[13] S. S. Zhang, L. G. Cao, U. Lombardo, E. G. Zhao, and S. G. Zhou, Phys. Rev. C **81**, 044313 (2010).
[14] S.-G. Zhou, J. Meng, P. Ring, and E.-G. Zhao, Phys. Rev. C **82**, 011301(R) (2010).
[15] B. Y. Sun and W. Pan, Nucl. Phys. A **909**, 8 (2013).
[16] R. F. Casten and B. M. Sherrill, Prog. Part. Nucl. Phys. **45**, S171 (2000).
[17] Y. A. Litvinov *et al.*, Phys. Rev. Lett. **95**, 042501 (2005).
[18] P.-G. Reinhard, Rep. Prog. Phys **52**, 439 (1989).
[19] P. Ring, Prog. Part. Nucl. Phys. **37**, 193 (1996).
[20] M. Bender, P.-H. Heenen, and P.-G. Reinhard, Rev. Mod. Phys **75**, 121 (2003).

[21] D. Vretenar, A. V. Afanasjev, G. A. Lalazissis, and P. Ring, Phys. Rep. **409**, 101 (2005).
[22] J. Meng, H. Toki, S. G. Zhou, S. Q. Zhang, W. H. Long, and L. S. Geng, Prog. Part. Nucl. Phys. **57**, 470 (2006).
[23] W. H. Long, N. Van Giai, and J. Meng, Phys. Lett. B **640**, 150 (2006).
[24] W. H. Long, H. Sagawa, N. V. Giai, and J. Meng, Phys. Rev. C **76**, 034314 (2007).
[25] J. D. Walecka, Ann. Phys. (NY) **83**, 491 (1974).
[26] B. D. Serot and J. D. Walecka, Adv. Nucl. Phys. **16**, 1 (1986).
[27] N. Paar, D. Vretenar, E. Khan, and G. Colò, Rep. Prog. Phys. **70**, 691 (2007).
[28] G. A. Lalazissis, S. Karatzikos, M. Serra, T. Otsuka, and P. Ring, Phys. Rev. C **80**, 041301 (2009).
[29] W. H. Long, P. Ring, N. Van Giai, and J. Meng, Phys. Rev. C **81**, 024308 (2010).
[30] W. H. Long, H. Sagawa, J. Meng, and N. Van Giai, Europhys. Lett. **82**, 12001 (2008).
[31] W. H. Long, T. Nakatsukasa, H. Sagawa, J. Meng, H. Nakada, and Y. Zhang, Phys. Lett. B **680**, 428 (2009).
[32] J.-P. Ebran, E. Khan, D. Pena Arteaga, and D. Vretenar, Phys. Rev. C **83**, 064323 (2011).
[33] L. J. Wang, J. M. Dong, and W. H. Long, Phys. Rev. C **87**, 047301 (2013).
[34] X. L. Lu, B. Y. Sun, and W. H. Long, Phys. Rev. C **87**, 034311 (2013).
[35] W. H. Long, H. Sagawa, J. Meng, and N. Van Giai, Phys. Lett. B **639**, 242 (2006).
[36] H. Liang, W. H. Long, J. Meng, and N. V. Giai, Eur. Phys. J. A **44**, 119 (2010).
[37] W. H. Long, P. Ring, J. Meng, N. Van Giai, and C. A. Bertulani, Phys. Rev. C **81**, 031302(R) (2010).

[38] H. Liang, N. Van Giai, and J. Meng, Phys. Rev. Lett. **101**, 122502 (2008).

[39] B. Y. Sun, W. H. Long, J. Meng, and U. Lombardo, Phys. Rev. C **78**, 065805 (2008).

[40] W. H. Long, B. Y. Sun, K. Hagino, and H. Sagawa, Phys. Rev. C **85**, 025806 (2012).

[41] J. Meng, Nucl. Phys. A **635**, 3 (1998).

[42] J. Dobaczewski, H. Flocard, and J. Treiner, Nucl. Phys. A **422**, 103 (1984).

[43] J. F. Berger, M. Girod, and D. Gogny, Comp. Phys. Comm. **63**, 365 (1991).

[44] J. Dobaczewski, W. Nazarewicz, T. R. Werner, J. F. Berger, C. R. Chinn, and J. Dechargé, Phys. Rev. C **53**, 2809 (1996).

[45] F. Chappert, M. Girod, and S. Hilaire, Phys. Lett. B **668**, 420 (2008).

[46] S. Goriely, S. Hilaire, M. Girod, and S. Péru, Phys. Rev. Lett. **102**, 242501 (2009).

[47] T. Gonzalez-Llarena, J. L. Egido, G. A. Lalazissis, and P. Ring, Phys. Lett. B **379**, 13 (1996).

[48] A. V. Afanasjev, T. L. Khoo, S. Frauendorf, G. A. Lalazissis, and I. Ahmad, Phys. Rev. C **67**, 024309 (2003).

[49] H. Kucharek and P. Ring, Z. Phys. A **339**, 23 (1991).

[50] J. Li, B. Y. Sun, and J. Meng, Int. J. Mod. Phys. E **17**, 1441 (2008).

[51] A. Bouyssy, J. F. Mathiot, N. Van Giai, and S. Marcos, Phys. Rev. C **36**, 380 (1987).

[52] L. P. Gorkov, Sov. Phys. JETP **7**, 505 (1958).

[53] S. G. Zhou, J. Meng, and P. Ring, Phys. Rev. C **68**, 034323 (2003).

[54] M. Bender, K. Rutz, P.-G. Reinhard, and J. A. Maruhn, Eur. Phys. J. A **8**, 59 (2000).

[55] J. Dobaczewski, P. Magierski, W. Nazarewicz, W. Satula, and Z. Szymanski, Phys. Rev. C **63**, 024308 (2001).

[56] W. Satuła, J. Dobaczewski, and W. Nazarewicz, Phys. Rev. Lett. **81**, 3599 (1998).

[57] G. F. Bertsch, C. A. Bertulani, W. Nazarewicz, N. Schunck, and M. V. Stoitsov, Phys. Rev. C **79**, 034306 (2009).

[58] J. F. Berger, M. Girod, and D. Gogny, Nucl. Phys. A **428**, 23 (1984).

[59] W. H. Long, J. Meng, N. Van Giai, and S. G. Zhou, Phys. Rev. C **69**, 034319 (2004).

[60] G. A. Lalazissis, T. Nikšić, D. Vretenar, and P. Ring, Phys. Rev. C **71**, 024312 (2005).

[61] A. V. Afanasjev and H. Abusara, Phys. Rev. C **81**, 014309 (2010).

[62] J. M. Yao, H. Chen, and J. Meng, Phys. Rev. C **74**, 024307 (2006).

[63] H. Chen, H. Mei, J. Meng, and J. M. Yao, Phys. Rev. C **76**, 044325 (2007).

[64] A. H. Wapstra, G. Audi, and C. Thibault, Nucl. Phys. A **729**, 129 (2003).

[65] S. Baroni, F. Barranco, P. F. Bortignon, R. A. Broglia, G. Colò, and E. Vigezzi, Phys. Rev. C **74**, 024305 (2006).

[66] D. M. Brink and R. A. Broglia, *Nuclear superfluidity: Pairing in finite systems* (Cambridge University Press, Cambridge, 2005), Vol. 24.

[67] R. A. Broglia, G. Potel, F. Barranco, and E. Vigezzi, J. Phys. G **37**, 064022 (2010).

[68] F. Barranco, R. A. Broglia, G. Gori, E. Vigezzi, P. F. Bortignon, and J. Terasaki, Phys. Rev. Lett. **83**, 2147 (1999).

[69] N. Giovanardi, F. Barranco, R. A. Broglia, and E. Vigezzi, Phys. Rev. C **65**, 041304(R) (2002).

[70] F. Barranco, P. F. Bortignon, R. A. Broglia, G. Colò, P. Schuck, E. Vigezzi, and X. Viñas, Phys. Rev. C **72**, 054314 (2005).

[71] E. V. Litvinova and A. V. Afanasjev, Phys. Rev. C **84**, 014305 (2011).

[72] J. L. Egido, P. Ring, S. Iwasaki, and H. J. Mang, Phys. Lett. B **154**, 1 (1985).

[73] J. Dobaczewski, M. V. Stoitsov, W. Nazarewicz, and P.-G. Reinhard, Phys. Rev. C **76**, 054315 (2007).

[74] A. Ozawa, T. Kobayashi, T. Suzuki, K. Yoshida, and I. Tanihata, Phys. Rev. Lett. **84**, 5493 (2000).

[75] P. Moller, J. R. Nix, W. D. Myers, and W. J. Swiatecki, At. Data Nucl. Data Tables **59**, 185 (1995).

[76] L. S. Geng, J. Meng, H. Toki, W. H. Long, and G. Shen, Chin. Phys. Lett **23**, 1139 (2006).

[77] F. Andreozzi, L. Coraggio, A. Covello, A. Gargano, and A. Porrino, Z. Phys. A **354**, 253 (1996).

[78] D. G. Fleming, J. Phys. **60**, 428 (1982).

[79] M. Jaminon and C. Mahaux, Phys. Rev. C **40**, 354 (1989).